THE ASTRONOMICAL JOURNAL VOLUME 80, NUMBER 8 AUGUST 1975

Study of the brightness and polarization structure of extragalactic radio sources

M. A. Stull,* K. M. Price, L. R. D'Addario,† S. J. Wernecke, W. Graf, and C. J. Grebenkemper
Radio Astronomy Institute, Stanford, California 94305
(Received 11 March 1975; revised 22 April 1975)

We have determined the brightness and linear polarization structure of 19 extended extragalactic radio sources at a frequency of 10.7 GHz and with a synthesized beam 17″ × 17″ csc δ. Compact components with self-absorption spectra coincident with the nucleus of an associated galaxy are fairly common, while many sources display regions of high-percentage polarization, sometimes greater than 40%. Comparison of our results with other studies, all at lower frequencies (generally ≤ 5 GHz), has yielded information on spectra, depolarization rates, and Faraday rotation of the polarization plane in various source regions. We can identify at least four distinct classes of extragalactic radio source. These classes form a sequence along which the prominence of the compact central component declines relative to that of the extended outer regions, while those outer regions become more ordered in their structure and assume specific polarization characteristics. We speculate that this sequence is in fact an evolutionary sequence.

INTRODUCTION

In spite of the development during the past decade of large aperture-synthesis radio telescopes, relatively few studies have been made, either of the overall structure of extragalactic sources at frequencies above 5 GHz or of the two-dimensional distribution of linearly polarized radiation at any frequency. Only high-frequency source maps will show the presence of compact regions with self-absorption spectra, while their comparison with lower-frequency maps will allow identification of old regions of sources where high-energy electrons have been depleted. Polarization measurements are crucial to any understanding of the origin and evolution of extragalactic radio sources. In an optically thin source of synchrotron radiation with a homogeneous magnetic field and an isotropic velocity distribution of the relativistic particles, the percentage of linear polarization is expected to be quite high (60%–80%), while the plane of polarization will be orthogonal to the magnetic field. Lower percentages of polarization are expected under less ideal circumstances, as when the magnetic field is twisted, when optically thick condensations are present, or when Faraday rotation is important; however, only the latter also causes frequency-dependent changes in the position angle of the observed polarization plane. In general, the detailed dependences of the degree of polarization and its position angle on frequency are expected to be fairly sensitive functions of physical conditions (magnetic field strength and orientation, electron density and energy distribution, etc.), and the determination of the variations of these parameters across a radio source should allow construction of an accurate source model.

We have used the Stanford University five-element interferometric radio telescope to produce two-dimensional maps of 16 extragalactic radio sources and one-dimensional (E–W) scans of three others at a frequency of 10.7 GHz. The sources were selected primarily on the basis of their brightness at 1.4 GHz; however, two sources, 3C 264 and 3C 390.3, were included because of their known low-frequency structure.

I. THE OBSERVATIONS

The Stanford telescope is an east–west rotation synthesis instrument whose main response has a half-peak width of approximately 17″×17″ csc δ at 10.7 GHz. The system noise temperature of 400 K combines with large effective collecting area (~380 m²) to give high sensitivity; point sources as weak as 0.015 f.u. (1 f.u. = 10^{-26} W m^{-2} Hz^{-1}) can be detected in a typical mapping period of 10 h. The Stanford telescope has been described in detail by Bracewell *et al.* (1973).

All observations were made with linearly polarized feed horns which were rotated every few minutes throughout the mapping period to position angles of 0°, 60°, and 120° (all position angles in this paper are measured east from north) with a sufficiently short cycle time to allow complete sampling of the aperture plane with each feed setting. Most sources were mapped twice to improve the signal-to-noise ratio and to provide a consistency check on the map reliability.

In addition to random receiver noise, a number of small systematic errors are believed to affect our data. These include small pointing and baseline errors, uncertainty in calibrator flux densities and polarizations (almost all suitable point sources are variable at 10.7 GHz), and uncertainty in the dependence of the antenna gains on zenith angle. The effects of most of these errors have been minimized by choosing calibrators for their proximity to the source being mapped. 10.7-GHz flux densities of calibrators measured with the 150-ft Algonquin telescope have been most generously supplied to us by Dr. Wilff Medd and Dr. Gladys Harvey of the National Research Council of Canada on a monthly

* Currently at NASA-Ames Research Center, Moffett Field, California.
† Currently at National Radio Astronomy Observatory, Charlottesville, Virginia.

basis. However, virtually all calibrator sources have polarized fluxes which are uncertain by up to a few percent of their total flux, and this uncertainty is greater than our instrumental polarization. Approximations in the data reduction process also contribute slightly to our polarization errors.

The following are good estimates for our combined random and systematic errors. On most of the maps the brightness error is ± 0.2 contour or less, while position errors for various features are ± 1.5 arcsec in right ascension and ± 1.5 csc δ arcsec in declination. The error in the percentage of linear polarization is $\pm 3\%$ in regions brighter than ~ 0.3 f.u./arcmin^2 and worse than this elsewhere, although for unresolved or slightly resolved sources it may be a little better. Similarly, the error in the position angle of the plane of polarization is smallest in regions where the polarized flux is high, and at best is about $\pm 10°$. Note that regions of low-percentage polarization may nevertheless contain significant ($\gtrsim 0.03$ f.u./arcmin^2) polarized flux, and the position angle there may be accurately determined. All 10.7-GHz error estimates in this paper refer to the standard deviation.

II. THE SOURCE MAPS

Figures 1–8 present two-dimensional maps of sources we have observed. Right ascension and declination are epoch 1950.0. The heavy curves are total-intensity brightness contours, while the lighter curves indicate the position angle of the polarization plane and are drawn so that the inclination of a tangent, as read with a protractor, is equal to the position angle of the direction of polarization at the point of tangency. On most maps the declination scale has been compressed to produce the appearance of a nearly circular beam. Note that the position angles appearing on the maps are the true angles and are not modified by the compression.

Shaded areas are regions where significant polarized flux has been detected; darker shading corresponds to a higher degree of polarization. Speckled areas are negative sidelobes. In unshaded positive regions, the total intensity is too low for that fraction which may be polarized to have been measured; in these regions the percentage polarization could be anywhere between 0% and close to 100%. Similarly, position-angle contours have been drawn only where we have detected significant polarized flux. The total-intensity contour interval and the percentage polarization indicated by a given degree of shading vary from map to map and are specified for each.

For three sources near the equator, 3C 270, 3C 348, and 3C 353, we are unable to obtain resolution in the north–south direction. One-dimensional (E–W) scans of total intensity, percent polarization, and position angle of the plane of polarization are displayed in Figs. 9–11.

All maps as presented here are based on the principal transfer function (Bracewell and Thompson 1973), and no attempt has been made to clean or otherwise alter them. However, in a number of cases we have used model-fitting and source-subtraction techniques (generally involving between two and four point sources) in an attempt to deduce structural features which are not immediately obvious from the principal solution; all subtractions were performed in the visibility domain. The specific results of this analysis are presented in the discussion of individual sources below; a general conclusion which we can state is that, at least for sources where the signal-to-noise ratio is high, the form and depth of the negative sidelobes which are produced by the principal transfer function method contain important information about source structure. Development of mathematical techniques by means of which this information can be presented in immediately comprehensible form is most desirable.

Spectral index α as used in this paper is defined by the relation $S_\nu \sim \nu^\alpha$, where S_ν is the flux density at frequency ν.

III. COMMENTS ON INDIVIDUAL SOURCES

3C 20 [Fig. 1(a)]: This is a double radio source with significant emission between the two components. Two faint galaxies (crosses) lie within this bridge, which has been resolved into two separate components by Branson *et al.* (1972) at 5.0 GHz. The percentage of polarization in the two main components increases to almost 20% in the regions nearest the central galaxies. Comparison of our results with the fluxes at 2.7 and 5.0 GHz of Branson *et al.* (1972) shows that the spectral indices of the two main components in the frequency interval 2.7–10.7 GHz are the same within the accuracy of the data and equal approximately -0.75.

3C 33 [Fig. 1(b)]: The source is associated with an elliptical galaxy (cross). It contains two components, the more southerly being substantially stronger and more highly polarized. Certain previous investigations have presented evidence for an additional source coincident with the central galaxy (Maltby and Moffet 1962; Fomalont 1968; MacDonald, Kenderdine, and Neville 1968), while Mitton (1970a), probably the most sensitive low-frequency (5 GHz) study of 3C 33, has found no evidence for such a component. Our map shows no identifiable peak in the vicinity of the galaxy, while there is a negative sidelobe nearby to the SE and another, more distant, to the NW. However, when two point-source responses of fluxes equal to those of the two main components and located at their respective positions are subtracted from the map, a significant peak does indeed appear at the position of the optical galaxy. We mapped 3C 33 on two separate days and this result is obtained independently for both sets of data. Furthermore, when we compute our instrumental response to two point sources of the appropriate intensities at the positions of the outer components, we find that the negative sidelobe to the SE of the optical galaxy extends across the position of the latter and

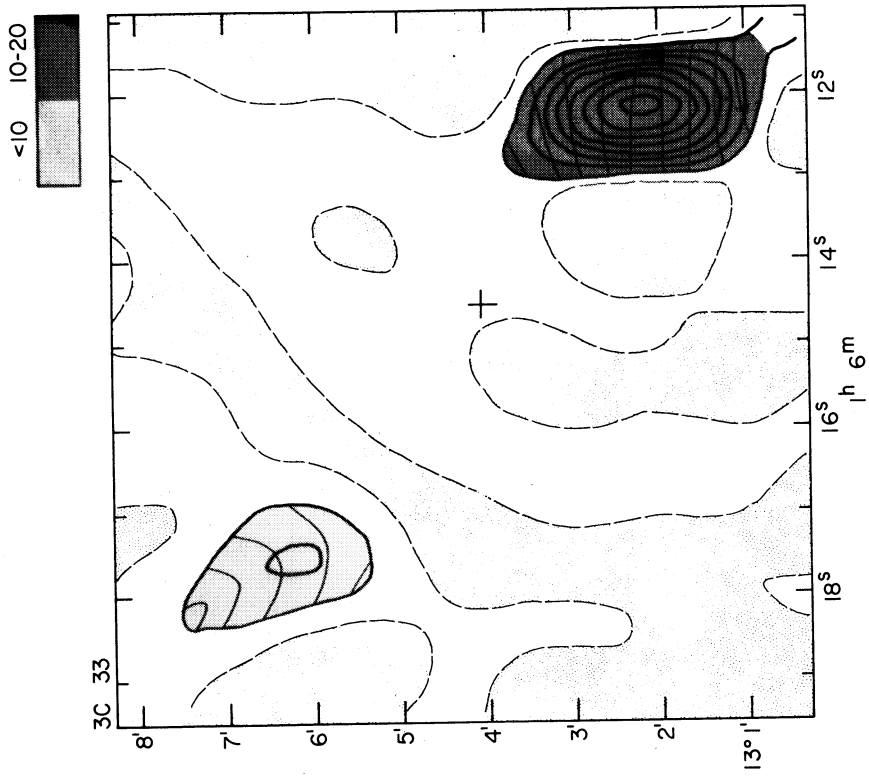

FIG. 1(b). 3C 33; Class IV-A. Contour interval 0.09 f.u./arcmin². Half-peak synthesized beamwidths 1.2ˢ in right ascension and 87 arcsec in declination.

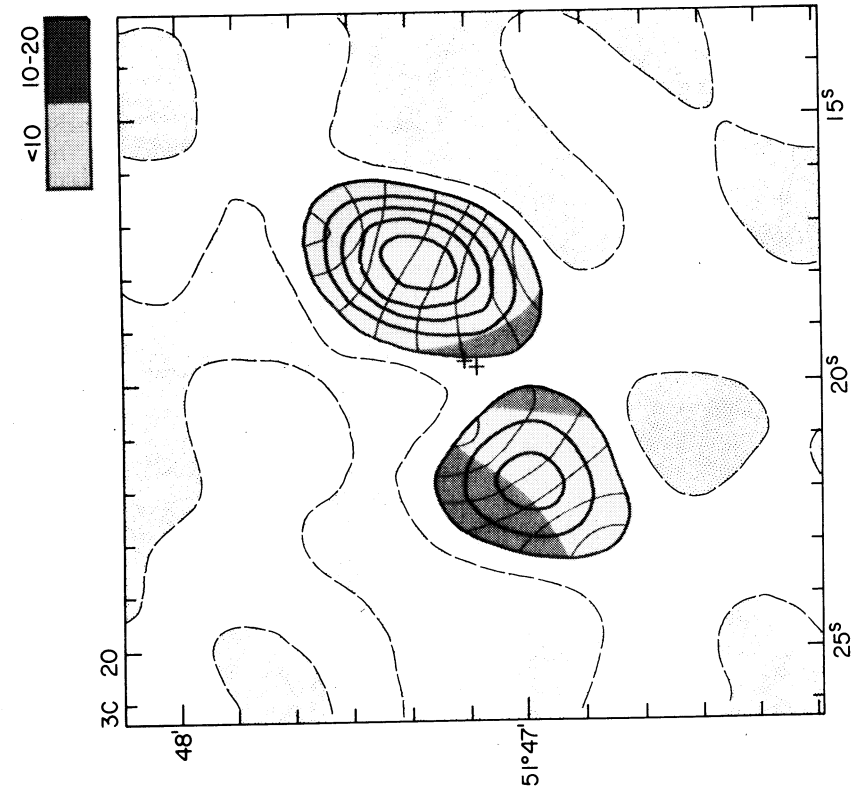

FIG. 1(a). 3C 20; Class IV-B. Contour interval 0.3 f.u./arcmin². Half-peak synthesized beamwidths 1.8ˢ in right ascension and 22 arcsec in declination.

TABLE I. Data for 3C 33.

	10.7-GHz flux (f.u.)	Spectral index	Polarization 10.7 GHz (%)	Polarization 2.8 GHz (%)	Polarization 1.4 GHz (%)	Position angle 10.7 GHz (deg)	Position angle 2.8 GHz (deg)	Position angle 1.4 GHz (deg)	Rotation measure (rad m^{-2})
SW	1.79±0.12	−0.67	14±3	8.1±1.4	10	93±14	88±10	62	∼−13
C	0.10±0.03	≳0	...	...	...	...	...	...	...
NE	0.68±0.06	−0.69	4±3	5.5±1.5	4	73±50	88±13	62	∼−7

joins with the negative sidelobe to the NW. On this basis we conclude that there is indeed a third, but very weak, component of 3C 33 coincident with the optical galaxy. Its flux density at 10.7 GHz is 0.10±0.03 f.u., and its 1950.0 right ascension and declination are $01^h06^m14.8^s\pm0.2^s$, 13°04′15″±13″, respectively; the corresponding coordinates of the galaxy are $01^h06^m14.54^s$, 13°04′14.75″ (Griffin 1963). From the failure of Mitton (1970a) to detect a strong source located at its position it may be presumed that the central component of 3C 33 has either a flat spectrum or one with a low-frequency cutoff.

The spectra of both outer components have been determined over the frequency interval 0.4–10.7 GHz by comparing our fluxes with those of Mitton (1970; 5 GHz) and MacDonald, Kenderdine, and Neville (1968; 0.4 and 1.4 GHz). The two spectra are identical to within the accuracy of the data, and may show slight curvature in the sense that they become steeper at higher frequencies. Measurements of the polarization of the two outer components have been obtained by Seielstad (1967) at 2.8 GHz, and by Seielstad and Weiler (1969) at 1.4 GHz. Neither component shows appreciable depolarization at lower frequencies, while the total rotation of the position angle also appears small. Flux, polarization, and spectral data for the three components of 3C 33 are summarized in Table I.

3C 66 [Fig. 2(a)]: This remarkable source contains two components, 3C 66A and B (Northover 1973) which do not seem to be related.

3C 66A is an unresolved and unidentified source about 6 arcmin northwest of 3C 66B. It exhibits a flat, quasar-like spectrum between 2.7 and 10.7 GHz; indeed, our 10.7-GHz flux is about 10% higher than that measured by Northover at 5 GHz. The percentage polarization of 3C 66A at 10.7 GHz is 3.8% ±1.7% in position angle 29°±13°. The low degree of polarization is typical of this type of radio source and is expected for an optically thick synchrotron emitter.

3C 66B is an extended and complex source at lower frequencies, with an intense core of emission which coincides with an elliptical galaxy, and a broad halo which extends primarily to the northeast and southwest. Northover (1973) has observed this source at 1.4, 2.7, and 5.0 GHz with an angular resolution appreciably better than ours. He found that the core source consisted of a central compact source in the galactic nucleus and a radio jet comprising several components and extending to the northeast, while the halo could be divided into three separate regions which exhibit fine structure and differing spectral indices. We have observed all four regions of 3C 66B. Comparison of our fluxes with Northover's results in an improved spectral index determination is summarized in Table II. The nomenclature for the source regions is Northover's.

It appears that the spectrum of the halo steepens at increasingly great distances from the core. The spectrum of the core itself is much flatter than at any point in the halo; in fact, at frequencies approaching 10 GHz and higher, its flux density may actually be increasing. Presumably this indicates the presence of a compact self-absorbed component within Northover's nuclear source. This interpretation is confirmed by the fact that on our map the position of the intensity peak is shifted notably to the southwest of that on Northover's 1.4-GHz map with comparable resolution; this shift is in the direction of the nucleus. We did not detect a significant polarized flux anywhere in 3C 66B. This is largely because the brightness of the halo is too low at 10.7 GHz to detect a fractional polarization smaller than 50%. However, the brightness of the core is quite high, and the percentage of linear polarization there must be less than 10%.

3C 98 [Fig. 2(b)]: 3C 98 is a double radio source, which, when observed with sufficiently high resolution, shows complex fine structure in both components (Branson *et al.* 1972). Our map does not resolve this fine structure; however, it does show pronounced "tails" extending inward from the two main lobes and toward the optical galaxy (cross). As in 3C 20, the degree of polarization increases markedly in these tails and approaches 30%. The position angle of the plane of polarization is noticeably different in the main components and varies considerably within the southwest lobe. Seielstad and Weiler (1969) also found that the degree of polarization reaches its maximum value in 3C 98 on the inside edges of the two components at 1.4 GHz; however, they report a peak of 13%. Thus it appears that appreciable depolarization takes place in these tails at frequencies below 10 GHz. The spectral indices of the two components between 2.7 and 10.7 GHz are about the same, −0.81 for the northeast lobe and −0.74 for the southwest lobe [based on 2.7- and 5.0-GHz fluxes from Branson *et al.* (1972)].

3C 111 [Fig. 3(a)]: One of the main results of the 10.7-GHz mapping program has been the discovery in many extended radio sources of centrally located components which exhibit a self-absorption spectrum.

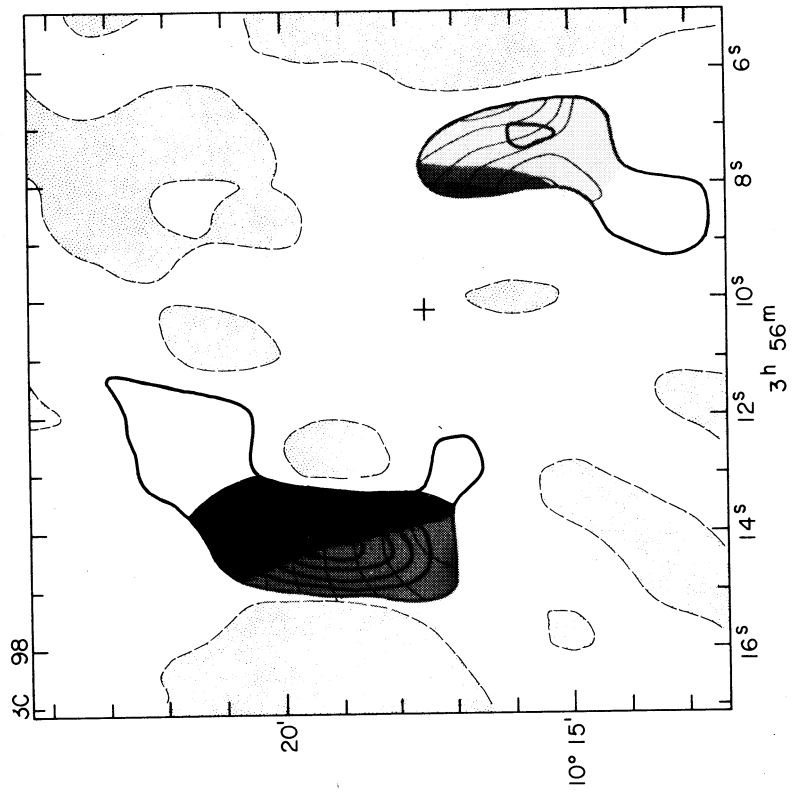

FIG. 2(b). 3C 98; Class IV-B. Contour interval 0.02 f.u./arcmin². Half-peak synthesized beamwidths 1.2ˢ in right ascension and 115 arcsec in declination.

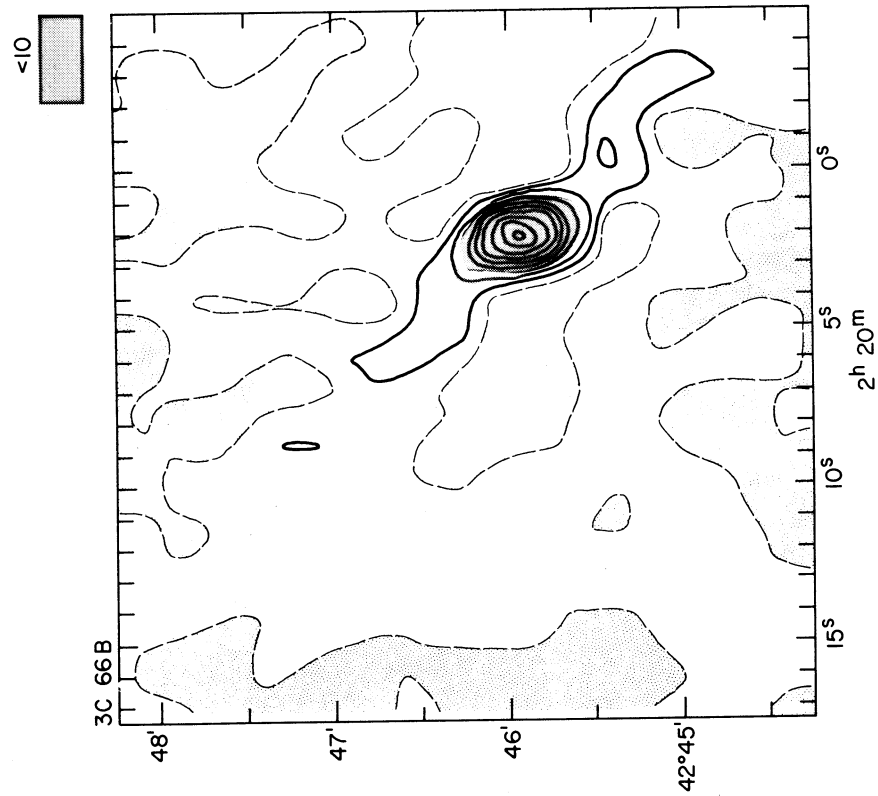

FIG. 2(a). 3C 66B; Class II. Contour interval 0.05 f.u./arcmin². Half-peak synthesized beamwidths 1.5ˢ in right ascension and 26 arcsec in declination.

TABLE II. Spectral index variation in 3C 66B.

	10.7-GHz flux (f.u.)	Spectral index
B1 (SW)	0.24±0.06	−0.63
B2 (core)	0.73±0.07	−0.22
B3 (NE)	0.15±0.05	−0.88
B4 (far NE)	0.29±0.06	−1.10

3C 111 has long been known to be a triple radio source in which the central component had a spectrum less steep than those of the two outer lobes (Mackay 1969; Mitton 1970b). Now at 10.7 GHz we have measured a flux density for this component which is more than 50% higher than that reported at 5.0 GHz (Mitton 1970b) and which implies that its spectrum turns sharply upward above 5 GHz. We have considerable confidence in this result since the fluxes we measure for the two outer components are consistent with their spectra between 0.4 and 5.0 GHz as reported by Mitton (1970b) to within the accuracy of the data, and actually fall marginally below their extension to 10.7 GHz.

Beyond this, the central component of 3C 111 is almost certainly variable, although we have not directly observed this. A search of the literature reveals that Bignell and Seaquist (1973) measured with a single dish a 10.7-GHz flux density of 3.37±.10 f.u. for 3C 111, while Kellermann and Pauliny-Toth (1973) measured 4.39±0.10 f.u. at the same frequency. Our combined flux for all three components is 5.49±0.29 f.u. Some of the discrepancy could result from uncertainty in the source-size correction applied to the single-dish measurements (although for the brightness distribution of 3C 111 this is likely to yield overestimates for the single-dish fluxes); however, we feel it more likely that variability of the central component accounts for most of it. Indeed, Fanaroff (1974) has reported direct evidence for variability at the 3-σ level in the central component of 3C 111 at 5 GHz.

The degree of polarization of the central component of 3C 111 is small, as would be expected for an opaque synchrotron source. The polarization of the outer components is appreciably greater. Seielstad and Weiler (1969) and Baldwin *et al.* (1970) have measured the polarization distribution in 3C 111 at 1.4 GHz, and it appears that the northeast component exhibits significant depolarization at frequencies below 10 GHz, although the southwest component does not. The rotation measure of the southwest component, however, may be larger than that of the northeast, although it is questionable that the differences in rotation measure here are significant. Data for the components of 3C 111 are summarized in Table III.

3C 123 [Fig. 3(b)]: Mitton (1970c) and Branson *et al.* (1972) have mapped 3C 123 at 5.0 GHz with higher resolution than we have used here. Their map shows an apparent double source surrounded by a weak halo. They did not obtain polarization data. We do not resolve the double structure; we do observe a halo extended to the northwest along the double-source axis, and one of lesser extent to the southeast. This halo is highly polarized, with the degree of polarization at 10.7 GHz exceeding 20% and possibly 30% at its northwest extremity. We note that the 5.0-GHz northwest component (Mitton 1970c; Branson *et al.* 1972) is much weaker and very much broader than that to the southeast and resembles the fine structure observed in the halo of 3C 66B (Northover 1973). It may be that it and 3C 123 are closely related.

3C 218 [Fig. 4(a)]: This source (Hydra A) appears single at our resolution. There seems to be a highly polarized halo, barely resolved, extending to the northeast.

3C 219 [Fig. 4(b)]: We here resolve five distinct source components showing varying degrees of polarization. Lower-frequency maps of 3C 219 do not approach our resolution, except for that by Branson *et al.* (1972) at 5.0 GHz (20-arcsec beam) which shows the same structure we find; nevertheless they do not provide data which would enable us to compute spectral indices for the highly polarized pair of inner lobes. Seielstad and Weiler (1969) have mapped the E–W polarization distribution in 3C 219 at 1.4 GHz; however, at their resolution the source is but double. Their results indicate that appreciable depolarization may occur in the northeast component between 10.7 and 1.4 GHz, but this conclusion should be regarded as tentative since their beam integrates over regions in which the position angle varies considerably.

The central source is coincident with a giant D galaxy, the brightest member of a cluster. As we lack spectral data, it is not possible to determine whether it is compact and opaque as in 3C 111; however, in view of the high degree of polarization which it exhibits, this is not likely. It is more probable that the central source comprises yet another pair of optically thin clouds on opposite sides of the D galaxy's center.

The northeast component is noticeably extended toward the east both on our map and on the 5.0-GHz map by Branson *et al.* (1972). The degree of polarization in this region does not seem to be significantly higher than in the rest of the component.

We summarize the data for the components of 3C 219 in Table IV.

3C 227 [Fig. 5(a)]: The source is a widely separated double source with two regions of marginally significant emission interior to the two main lobes. In addition the west lobe is quite broad with low brightnesss, which makes it relatively inconspicuous on our map (R.A. $\sim 9^h45^m00^s$), while the east component is more compact and considerably brighter. Only the east component is bright enough for us to determine its polarization distribution; the degree of polarization is slightly less than 20% throughout. Seielstad and Weiler (1971) have observed the distribution of polarized radiation in 3C 227 at 1.4 and 2.9 GHz. Their results show that the east

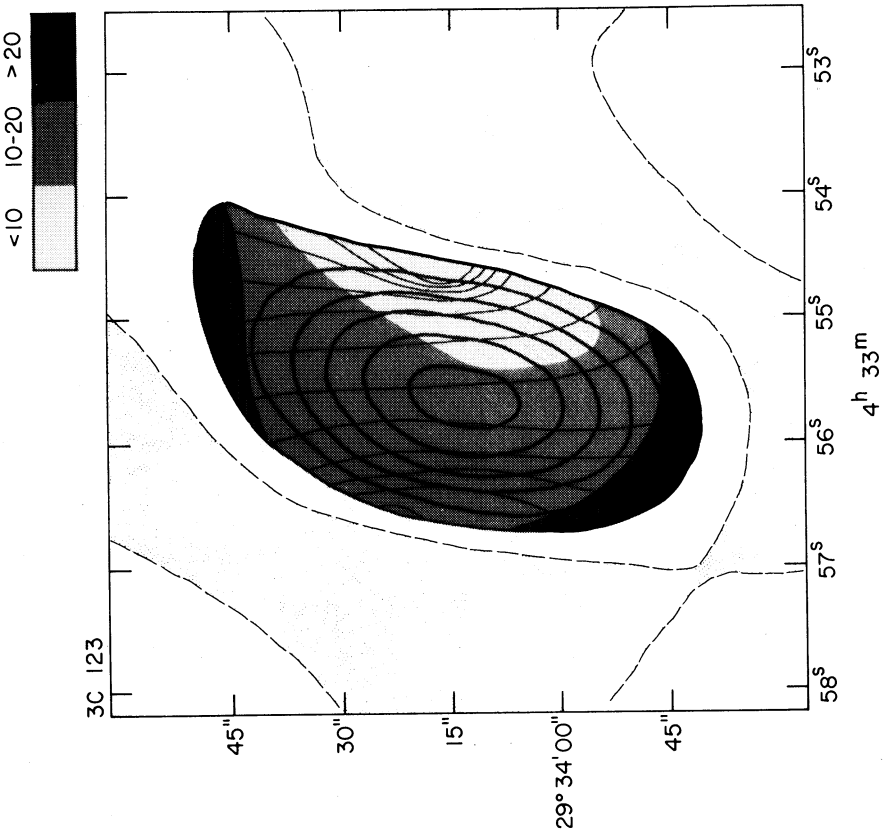

FIG. 3(b). 3C 123; Class II. Contour interval 4.0 f.u./arcmin². Half-peak synthesized beamwidths 1.3ˢ in right ascension and 37 arcsec in declination.

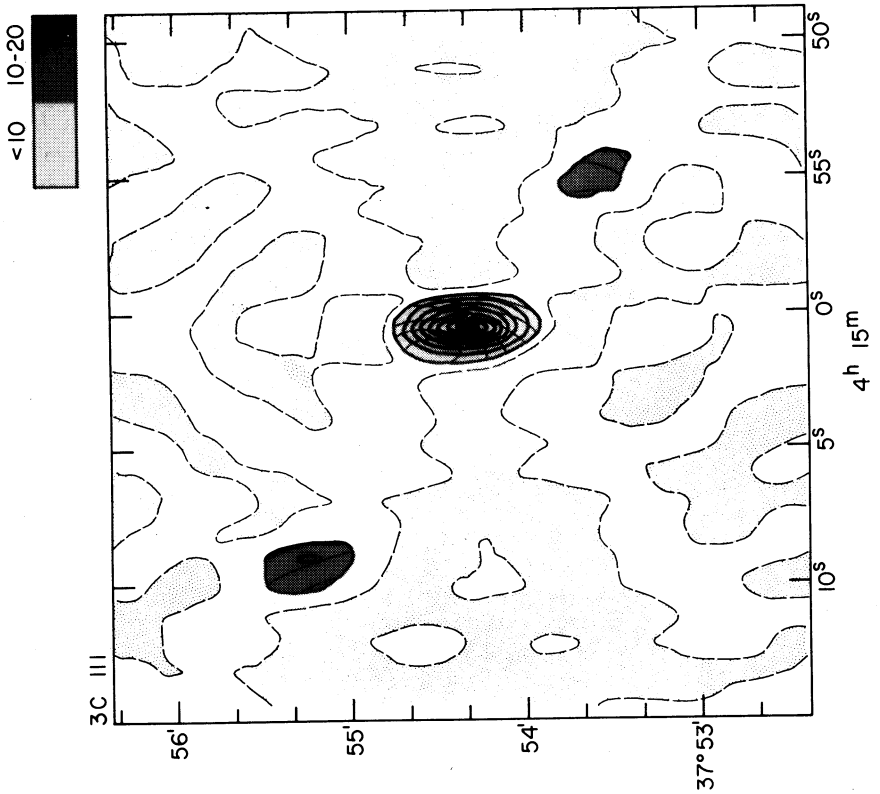

FIG. 3(a). 3C 111; Class III. Contour interval 0.5 f.u./arcmin². Half-peak synthesized beamwidths 1.4ˢ in right ascension and 28 arcsec in declination.

TABLE III. Data for 3C 111.

	10.7-GHz flux (f.u.)	Spectral index	Polarization 10.7 GHz (%)	Polarization 1.4 GHz (%)	Position angle 10.7 GHz (deg)	Position angle 1.4 GHz (deg)	Rotation measure (rad m^{-2})
SW	1.05±0.07	−0.75	11.3±2.5	9.2±1	15±20	67±3	∼21
C	3.22±0.19	−0.35 below 5 GHz +0.63 above 5 GHz	4.8±2.5	4.5±3	177±50	130±30	∼−19
NE	1.22±0.09	−0.76	17.8±2.5	5.5±0.7	26±13	32±5	∼2

component has a slightly higher degree of polarization at 2.9 GHz than at 1.4 GHz; however, their 2.9-GHz results and ours at 10.7 GHz are virtually identical, indicating no depolarization over this frequency interval. There is little or no rotation of the polarization plane in the east component between 1.4 and 10.7 GHz.

3C 264 [Fig. 5(b)]: This is a remarkable source with structure similar to that noted in 3C 66B and probably also to 3C 274 (see below). We call attention to the halo-type structure surrounding the source and note that, as in 3C 66B, the halo is not symmetrical, but has a pronounced, jet-like extension toward the northeast. Again as in 3C 66B, the halo spectrum appears to steepen at increasing distances from the core; MacDonald, Kenderdine, and Neville (1968) have reported a pronounced decrease in the size of 3C 264 between 0.4 and 1.4 GHz, and this decrease continues to 10.7 GHz. We have been able to measure the degree of polarization in the northeast halo over much of its extent, and find that it increases at increasing distances from the core, ultimately reaching extremely high values (∼35%–40%). According to Seielstad and Weiler (1969), the polarization of this region of the source is less than 10% at 1.4 GHz, so a pronounced depolarization, and one of the largest of which we are aware, evidently occurs at frequencies below 10.7 GHz.

3C 270 [Fig. (9)]: 3C 270 is associated with a giant elliptical galaxy, NGC 4261, in the Virgo cluster, and has very large angular extent (∼10 arcmin). Due to its proximity to the celestial equator, we obtain only east–west resolution with our interferometer. The source is a radio double. Both lobes show extended emission "tails" toward the central galaxy on their interiors. Over the main portion of both lobes the degree of polarization is relatively low, varying between 20% and less than 5%; however, in the inner "tails" it becomes very high and exceeds 40% [Figs. 9(a) and 9(b)].

Since 3C 270 is of such large angular extent, the comparison of its polarization distribution at several frequencies is of great interest. Seielstad and Weiler (1971) have obtained east–west maps of linear polarization in 3C 270 at 1.4 and 2.9 GHz with resolution somewhat poorer than ours. Comparison of our data with theirs shows significant differences in the depolarization between the two components. For the west component the degree of polarization in the tail at 2.9 GHz (∼30%) is only slightly less than at 10.7 GHz. Between the tail and the intensity peak, the degree of polarization at all three frequencies is about the same (∼10%), while toward the component's sharp western edge, depolarization at lower frequencies is again evident, but now occurs principally between 10.7 and 2.9 GHz. In the east component, on the other hand, depolarization is evident only in the tail, where it occurs entirely between 10.7 (>40%) and 2.9 GHz (∼15%); elsewhere in the component the degree of polarization is essentially the same at all three frequencies.

There is considerable rotation of the plane of polarization across 3C 270. It is evident from Fig. 9(c) that the rotation measure and intrinsic position angle vary in a similar manner as one goes outward across both components. Over most of the source the rotation measure is negative (position angle rotates from S to E to N with increasing wavelength). We note that significant depolarization does not occur in those regions of both components where R.M. $\lesssim -20$ rad m^{-2}.

Very prominent on our map is a bright, compact source coincident with the nucleus of NGC 4261, although the integrated flux density of the outer lobes at 10.7 GHz exceeds that of the central source by an order of magnitude due to their large angular extent. As this source does not appear in the data of Seielstad and Weiler (1971), we conclude that its spectrum is cut off below 10.7 GHz in the manner of an opaque synchrotron source; its 10.7-GHz flux density is 0.30±0.02 f.u., and it does not show detectable linear polarization (upper limit 10%). We note that the intrinsic luminosity of this source at 10.7 GHz is virtually identical to that of the compact nuclear source in Centaurus A (Price and Stull 1973) at the same frequency. The latter is one of the most unusual compact sources yet discovered (Kellermann 1974; Grindlay *et al.* 1975) in that it exhibits an extremely high turnover frequency (∼30 GHz), may vary on a time scale of a few days at millimeter wavelengths, and appears to be a source of both x-rays and very-high-energy gamma rays ($h\nu \sim 10^{11}$ eV). We speculate that the 3C 270 source may have similar characteristics. However, we observed it several times between October 1973 and May 1974 and found no evidence for variability exceeding 20% at 10.7 GHz.

3C 274 [Fig. 6(a)]: 3C 274 (Virgo A) was one of the first radio sources discovered and remains one of the most interesting. The map which we present here covers the central regions of the optical galaxy M87. It shows a double source with one component lying along the

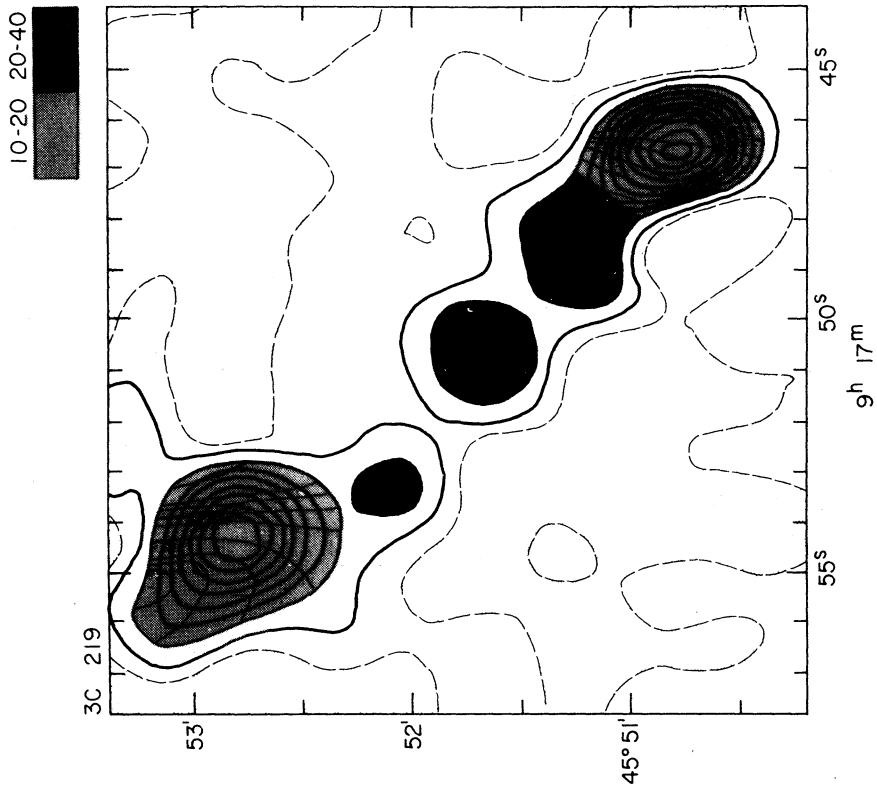

FIG. 4(b). 3C 219; Class IV. Contour interval 0.04 f.u./arcmin². Half-peak synthesized beamwidths 1.6^s in right ascension and 25 arcsec in declination.

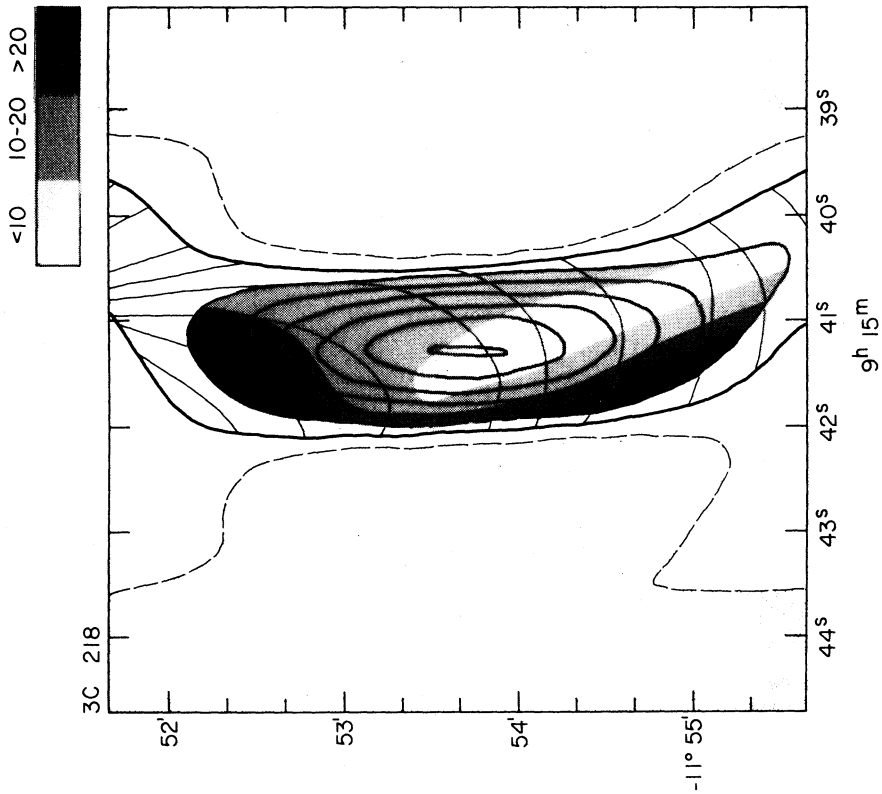

FIG. 4(a). 3C 218; Class II. Contour interval 0.6 f.u./arcmin². Half-peak synthesized beamwidths 1.2^s in right ascension and 115 arcsec in declination.

TABLE IV. Data for 3C 219.

	10.7-GHz flux (f.u.)	Polarization 10.7 GHz (%)	Polarization 1.4 GHz (%)	Position angle 10.7 GHz (deg)	Position angle 1.4 GHz (deg)
NE (outer)	0.52±0.02	13.3±2.2	...	30±14	...
NE (inner)	0.09±0.02	34 ±9	...	179±23	...
NE (combined)	0.61±0.02	14.3±3.0	1.2	21±17	146
C	0.15±0.02	31 ±6	...	28±14	...
SW (inner)	0.15±0.02	23 ±5	...	60±20	...
SW (outer)	0.39±0.02	12.5±2.2	...	165±14	...
SW (combined)	0.54±0.02	4.7±2.9	7.5	6±17	112

famous optical jet (indicated on map), and the other in the direction of the counterjet reported by Arp (1967). A map with somewhat better resolution at 5 GHz (Graham 1970) shows triple structure, with the third source located just south of the optical nucleus (cross), while the other two sources are located at a somewhat greater separation than our map indicates. These differences are due entirely to the differences in the resolving powers of the instruments used. When we compute our response to the brightness distribution described by Graham, we get virtually the same map we present here.

The compact source structure in the nucleus of M87 is, as has long been known, surrounded by a broad halo. At 10.7 GHz we observe this halo; however, it is smaller than one-quarter the size determined for it by Seielstad and Weiler (1969) at 1.4 GHz. Thus we see here a phenomenon similar to that in 3C 66B and 3C 264 where the halo shrinks markedly as the observing frequency is increased. For 3C 66B we were able to determine directly from the measured fluxes that the halo spectrum becomes steeper at increasing distances from the central core, and this must be true for 3C 264 and 3C 274 as well.

At 10.7 GHz the degree of polarization of the radio source associated with the optical jet is 7% or 8%, while that of the source coincident with the counterjet appears to be less than 5%. Hiltner (1959), using photoelectric photometry, found that the most westerly of the three optical condensations in the jet was 20.7% polarized in position angle 133°.8; the middle condensation was 23.2% polarized in position angle 37°.1; and the degree of polarization of the easternmost condensation was 11.1% in position angle 125°.8. Caution should be observed before interpreting these results as implying a substantial depolarization between optical and radio wavelengths, however, as Hiltner's resolution was appreciably higher than ours and the position angles of the optical polarization vary considerably.

The degree of polarization increases in the halo and approaches 20% at the greatest distances from the core where we have determined it. At 1.4 GHz Seielstad and Weiler (1969) found an integrated polarization of 1.6% for the halo and less than 0.1% for the core. Our map has been made with higher resolution and shows considerable variation in the position angle of the plane of polarization over both core and halo. This accounts for at least part of the reduction in the percentage of polarization reported at 1.4 GHz. However, it is possible that an appreciable depolarization nevertheless occurs at frequencies below 10.7 GHz, especially in the halo.

3C 348 (Fig. 10): 3C 348 (Hercules A) is a classical double radio source. The west component is moderately polarized (15%–20%) at 10.7 GHz, and its spectrum is significantly steeper than that of the eastern component. According to the data of Seielstad and Weiler (1971), almost total depolarization occurs between 10.7 and 2.9 GHz; it is perhaps significant that the rotation measure for this component appears to be quite large. The more intense eastern component exhibits notable variations in degree of polarization. These are very similar to what is observed in the components of other radio doubles such as 3C 20, 3C 98, 3C 219, and 3C 270. The polarization is low (<10%) at the component's sharp outer edge, but increases to nearly 30% at the inner edge, which is not sharp, but forms an extended tail stretching toward the source center. In 3C 348, however, the tail is less pronounced and the component profile more symmetrical than in other double sources. According to Seielstad and Weiler (1971) the tail of the east component of 3C 348 is only about 10% polarized at 2.9 GHz, and this drops further to about 3% at 1.4 GHz; however, the degree of polarization of its east edge is similar at all three frequencies.

3C 353 (Fig. 11): This is an unusual radio double with, at least among our sample of sources, unique polarization features. The chief abnormality is seen in the eastern component. Most double-source components are characterized by a sharp, relatively unpolarized outer edge, and an inwardly extended and highly polarized tail. Here we do observe the highly polarized tail (~30%), but we also observe another region of even higher polarization (~35%) lying to the east of the component's point of peak intensity. The polarization of the intensity peak itself is quite low (~5%), and the degree of polarization falls again to near zero near the eastern (outer) edge which, however, is anything but sharp. The western component of 3C 353 appears more "normal," exhibiting a very highly polarized (~40%) inner tail and about 15% polarization elsewhere. The east lobe resembles what might be produced if a typical component with a slightly polarized outer edge and

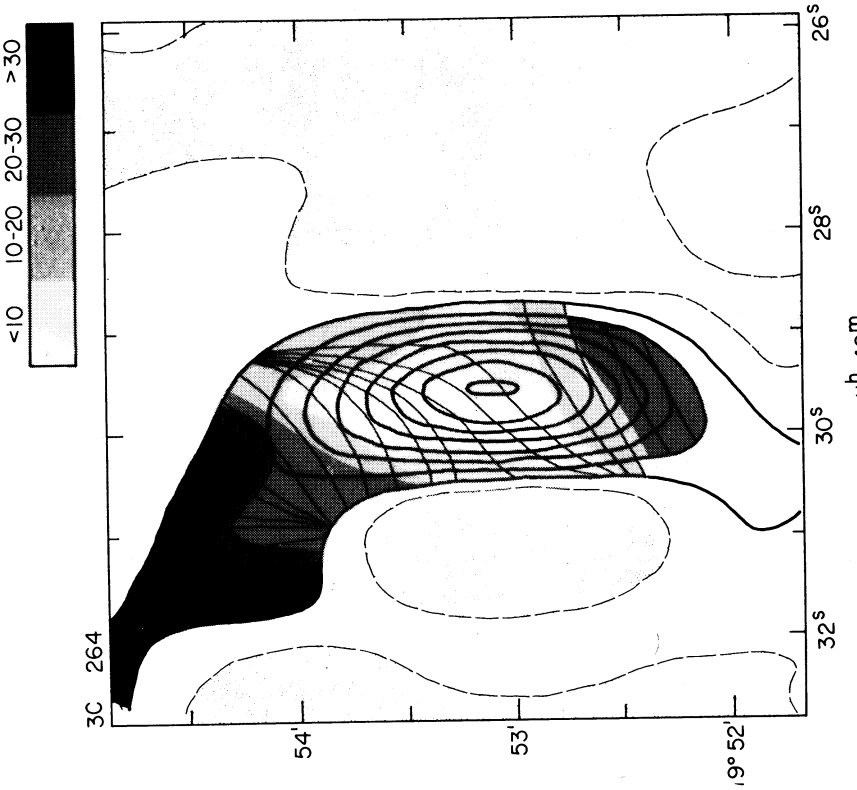

FIG. 5(b). 3C 264; Class II. Contour interval 0.08 f.u./arcmin². Half-peak synthesized beamwidths 1.2^s in right ascension and 58 arcsec in declination.

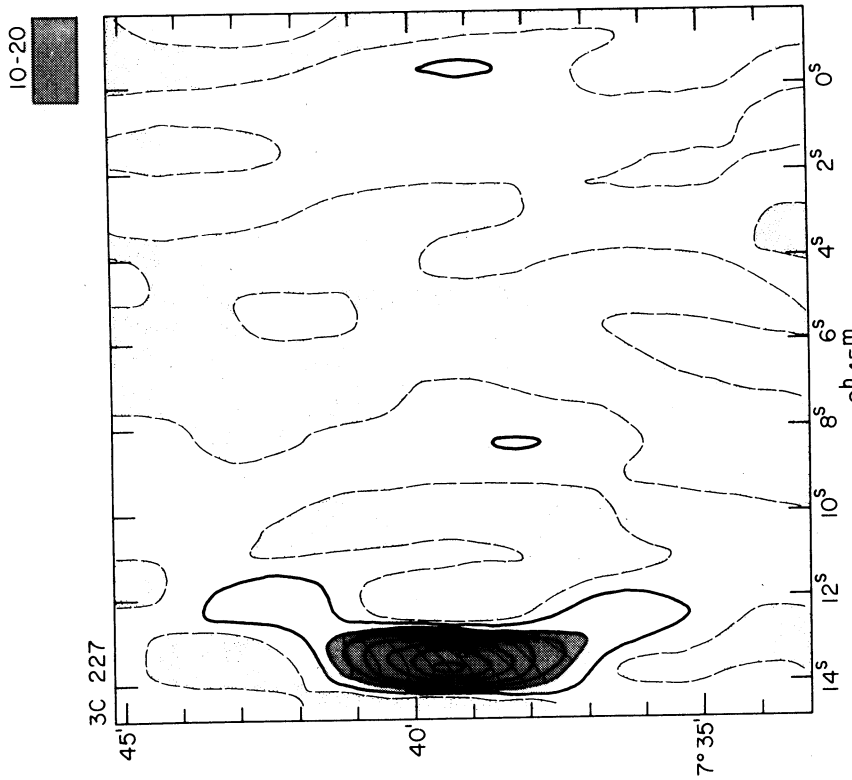

FIG. 5(a). 3C 227; Class IV-B. Contour interval 0.008 f.u./arcmin². Half-peak synthesized beamwidths 1.1^s in right ascension and 150 arcsec in declination.

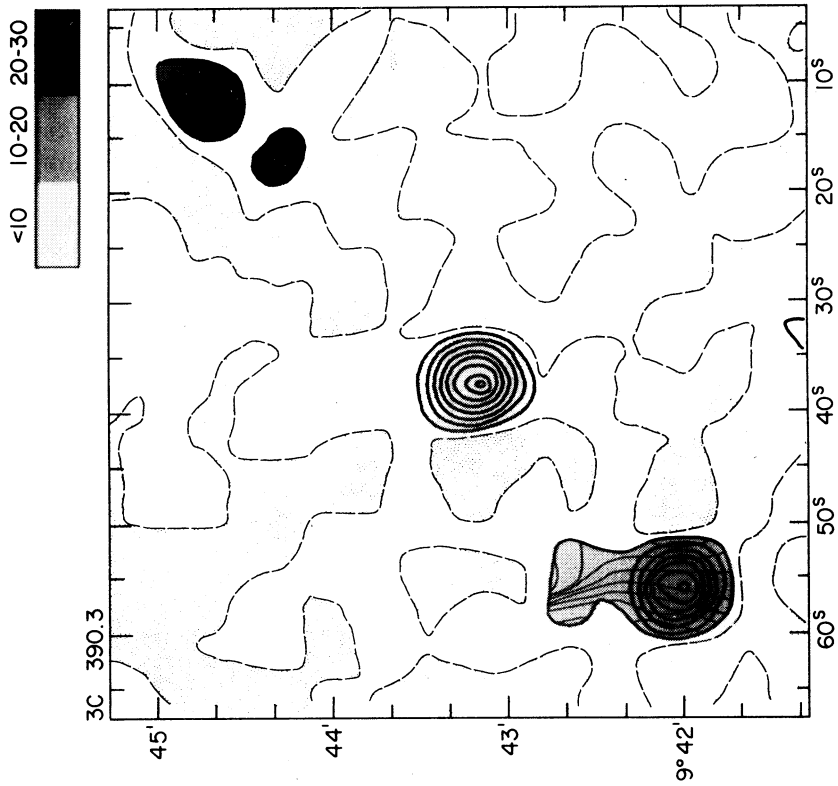

FIG. 6(b). 3C 390.3; Class III. Contour interval 0.25 f.u./arcmin². Half-peak synthesized beamwidths 6.4ˢ in right ascension and 18 arcsec in declination.

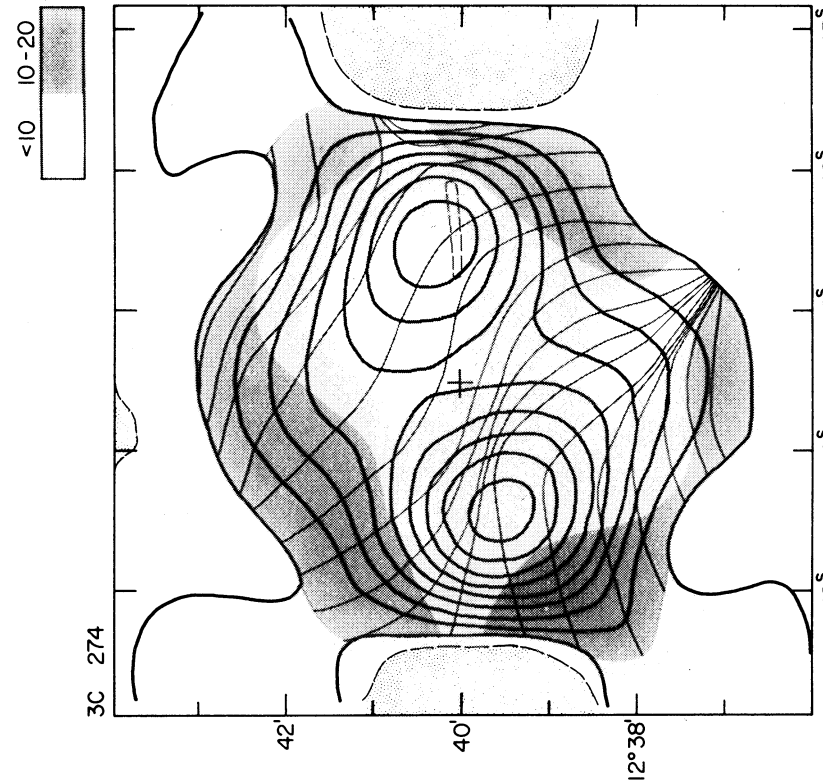

FIG. 6(a). 3C 274; Class II. Contour interval 0.35 f.u./arcmin². Half-peak synthesized beamwidths 1.2ˢ in right ascension and 90 arcsec in declination.

TABLE V. Data for 3C 390.3.

	10.7-GHz flux (f.u.)	Spectral index	Polarization 10.7 GHz (%)	Polarization 5.0 GHz (%)	Polarization 2.7 GHz (%)	Position angle 10.7 GHz (deg)	Position angle 5.0 GHz (deg)	Position angle 2.7 GHz (deg)
N	0.46±0.03	−0.85	21.1±2.8	19 ±6	10.5±3	36±11	55±20	37±15
C	0.83±0.04	+0.65	3.5±2.3	<4	<4	141±60	...	...
S	1.04±0.05	−0.86	12.0±2.2	13.3±1.5	14.7±1	4±16	171±7	171±4
Diffuse emission	~0.2	−1.33	...	...	...	...	...	...

heghly polarized inner tail were overtaken by a subsiquently ejected cloud with similar properties, but the lack of evidence for a double ejection on the west side of the source causes us to doubt that this is a correct explanation.

At lower frequencies only the inner tail of 3C 353's western component appears to be appreciably polarized —15% at both 2.9 and 1.4 GHz (Seielstad and Weiler 1971)—but this is much less than its 10.7-GHz value. Thus, except in the region of the eastern intensity peak and the extreme eastern source edge, appreciable depolarization takes place in 3C 353 between 10.7 and 2.9 GHz, while little more occurs between 2.9 and 1.4 GHz.

3C 390.3 [Fig. 6(b)]: This source is virtually identical to 3C 111. It, too, is triple and the flux density of the central component (which coincides with an N galaxy) rises at higher frequencies in the manner of an opaque synchrotron source. The spectral indices of the outer components are nearly identical, and their polarization moderately high. As in 3C 111 one component shows no significant depolarization at lower frequencies, whereas the other does. No significant rotation of the plane of polarization is observed in either component. There is a very faint diffuse emission between the outer components and the central source; the spectrum of this radiation is considerably steeper than in other source regions.

The data for 3C 390.3 are summarized in Table V. The spectral indices are for the frequency range 0.4–10.7 GHz, except for the central component where it is for 2.7–10.7 GHz. The fluxes and polarizations at 2.7 and 5.0 GHz are due to Harris (1972), while the fluxes at 0.4 and 1.4 GHz are from MacDonald, Kenderdine, and Neville (1968).

3C 405 [Fig. 7(a)]: The first extragalactic radio source to be discovered, 3C 405 (Cygnus A), has been the subject of several high-resolution studies, notably by Mitton (1971) at 5.0 GHz, Bing and Seielstad (1972) at 8.3 and 9.6 GHz, and Hargrave and Ryle (1974) at 5.0 GHz, and all have mapped the polarization distribution as well as that of the total brightness. In spite of the fact that rotation measures in 3C 405 appear to be huge in places, the four-frequency data now available should make possible their ambiguity-free determination across the source, and a calculation of depolarization rates as well. This in turn could lead to a detailed understanding of the magnetic field structure in addition to some insight into the properties of the particles which compose the radio-emitting clouds. However, we do not undertake such an analysis in this paper.

Hargrave and Ryle (1974) have presented evidence for the existence of a compact radio source coincident with the central galaxy of Cygnus A. We do not detect this source and place an upper limit of 3 f.u. on its 10.7-GHz flux density.

Finally, we note that in 3C 405, as in other double radio sources, we observe highly polarized tails extending inward from the two main lobes toward the central galaxy.

3C 409 [Fig. 7(b)]: We barely resolve this source. As mapped with the principal transfer function 3C 409 appears single; however, we have computed the response of our instrument to possible models for it and find we can reproduce our sidelobe structure most closely with a double-source model, where two components of equal intensity are separated by perhaps 15–20 arcsec along the apparent NW–SE source axis (P.A. 150°). The polarization is uniformly low and its position angle fairly constant throughout the emitting region.

3C 433 [Fig. 8(a)]: Again, this source is one which we barely resolve. However, we do detect a small halo extended to the west and northwest of the source, and possibly also to the north and northeast. This feature has also been detected by Branson *et al.* (1972) at 5.0 GHz. Our results show that at 10.7 GHz it is highly polarized, especially to the west where the degree of polarization exceeds 20%. As we have noted in other sources with core–halo structure, there are pronounced variations in the position angle of the plane of polarization across 3C 433.

3C 452 [Fig. 8(b)]: This source resembles 3C 270 in its main characteristics. It is a typical radio double with an additional central compact source coincident with a giant elliptical galaxy, and emitting only a small fraction of the total 10.7-GHz flux. The compact source exhibits the rising spectrum at higher frequencies typical of opaque synchrotron emitters and a slight degree of polarization, while the main lobes possess highly polarized tails extending inward. Riley and Branson (1973) have mapped the polarization distribution in 3C 452 at 2.7 and 5.0 GHz, while it has been determined at 1.4 GHz by Baldwin *et al.* (1970). Com-

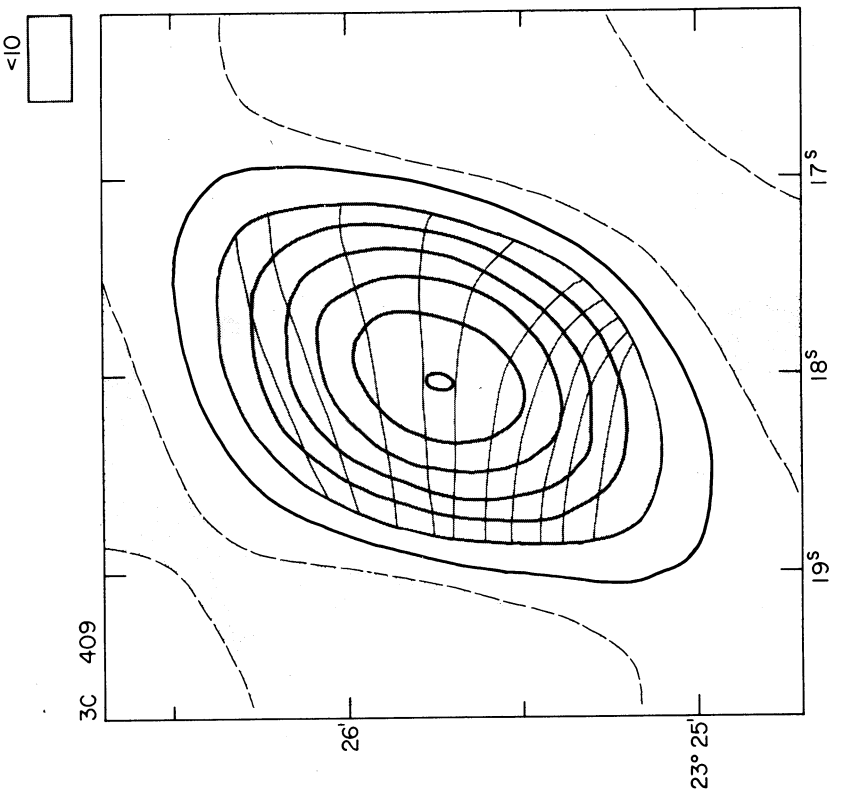

FIG. 7(b). 3C 409; Class IV. Contour interval 0.15 f.u./arcmin². Half-peak synthesized beamwidths 1.2s in right ascension and 47 arcsec in declination.

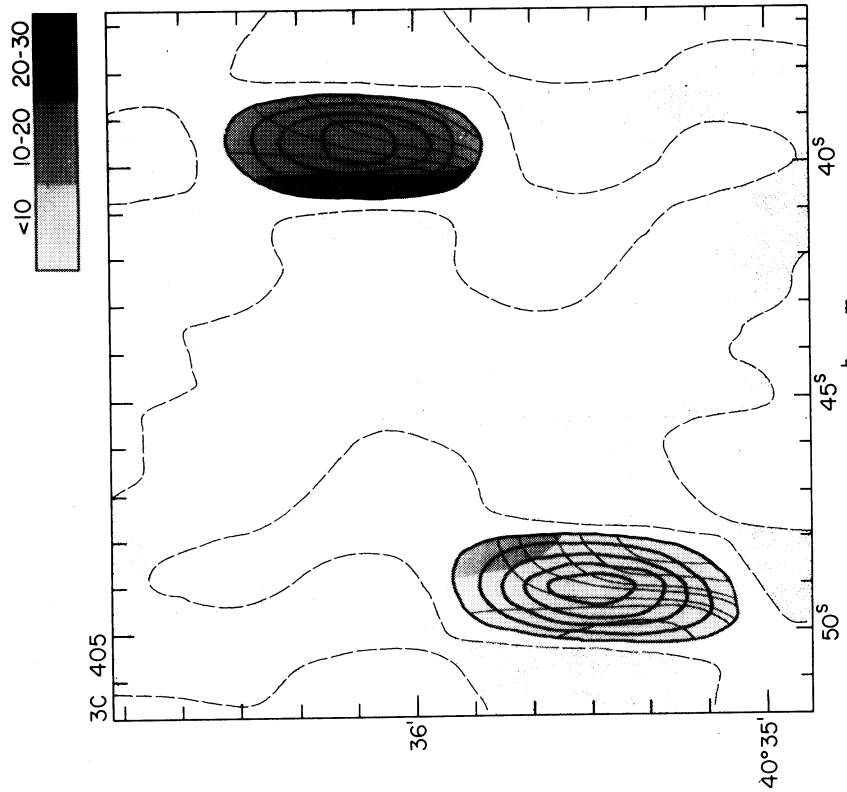

FIG. 7(a). 3C 405; Class IV-A. Contour interval 20.0 f.u./arcmin². Half-peak synthesized beamwidths 1.5s in right ascension and 27 arcsec in declination.

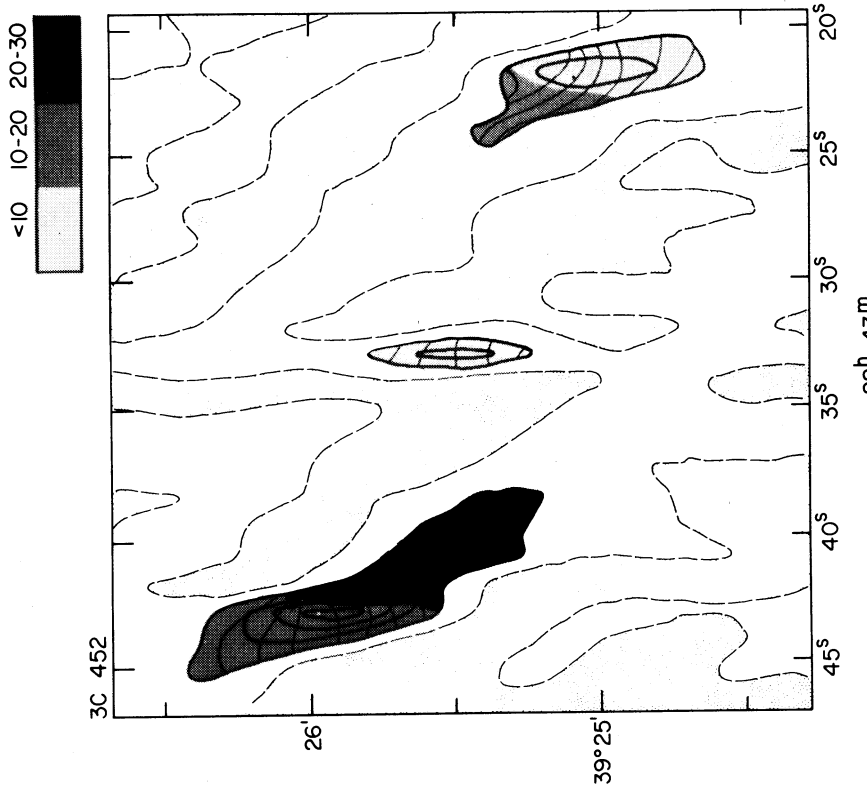

FIG. 8(b). 3C 452; Class IV-A. Contour interval 0.12 f.u./arcmin². Half-peak synthesized beamwidths 1.5° in right ascension and 28 arcsec in declination.

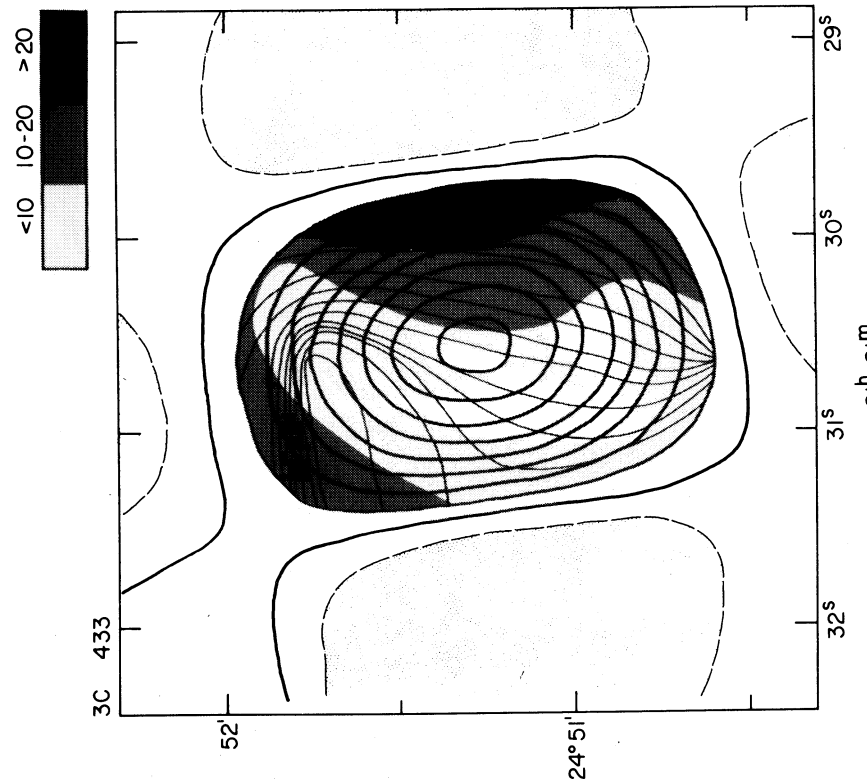

FIG. 8(a). 3C 433; Class II. Contour interval 0.15 f.u./arcmin². Half-peak synthesized beamwidths 1.2° in right ascension and 45 arcsec in declination.

parison of our data with theirs shows that at most slight depolarization takes place in the tail of the east component between 10.7 and 1.4 GHz, while in the tail of the west lobe depolarization occurs primarily between 2.7 and 1.4 GHz. On the other hand, an appreciable depolarization occurs in the main part of the east lobe between 10.7 and 5.0 GHz, although not in the west lobe.

The data for 3C 452 are summarized in Table VI.

IV. DISCUSSION

One of the main differences between our maps at 10.7 GHz and those of comparable resolution at lower frequencies is that quite often the degree of polarization in extended source components is higher at 10.7 GHz; seldom or never is it substantially and significantly lower than at lower frequencies, though it may be comparable. This can be understood if the depolariza-

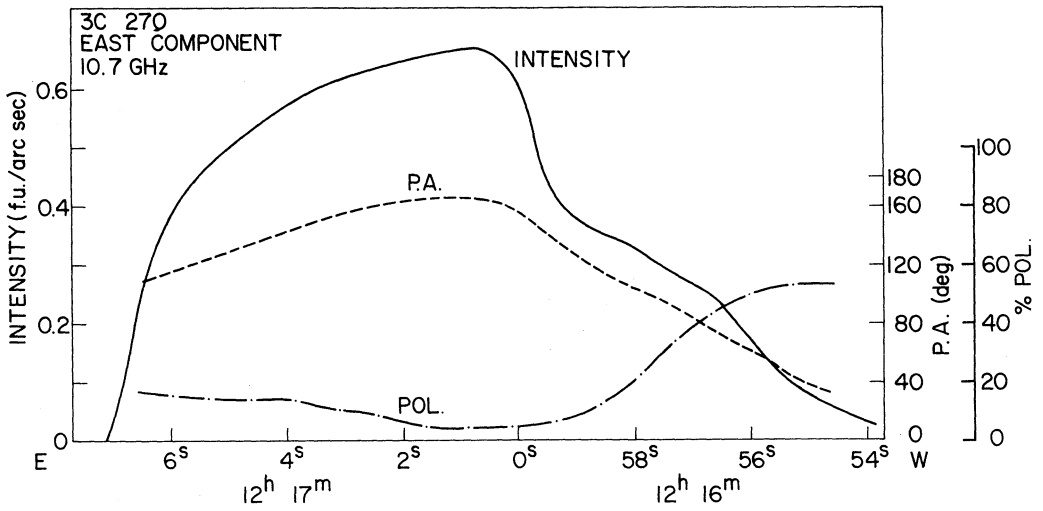

FIG. 9(a). 3C 270; Class IV-A. East component: Intensity, percent polarization, and position angle. Half-peak synthesized beamwidth 1.1s in right ascension.

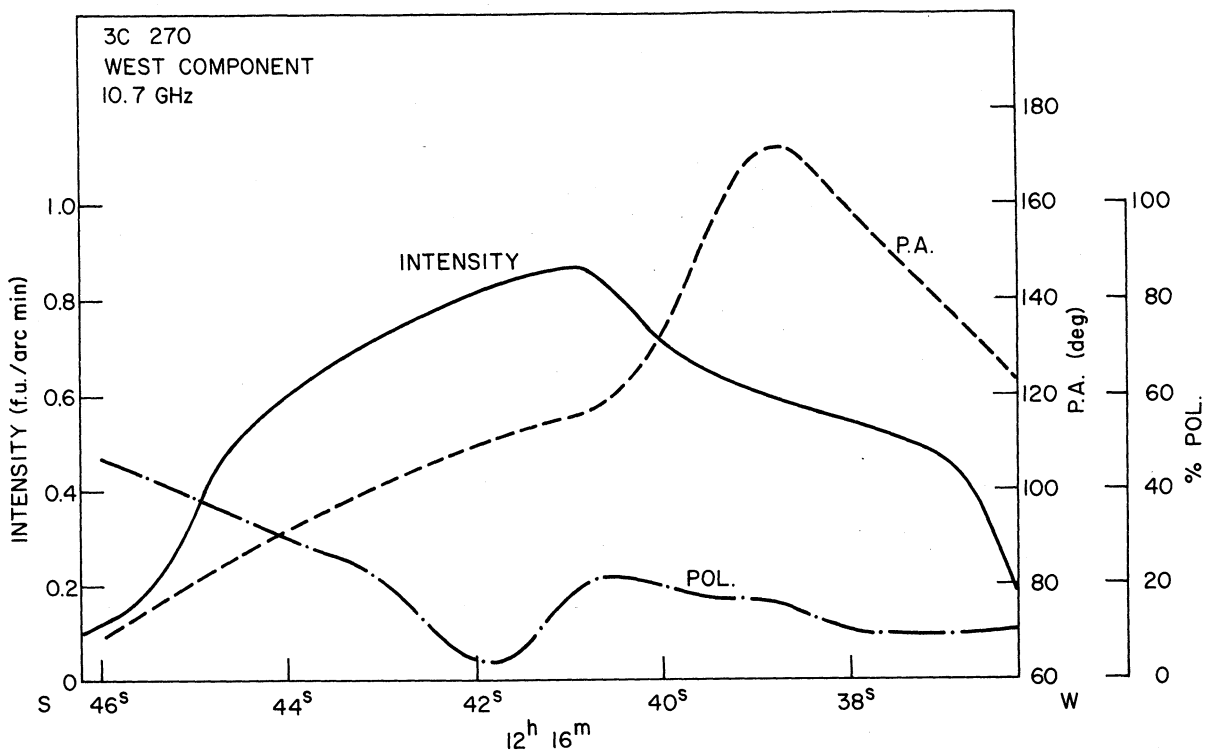

FIG. 9(b). 3C 270; Class IV-A. West component: Intensity, percent polarization, and position angle. Half-peak synthesized beamwidth 1.1s in right ascension.

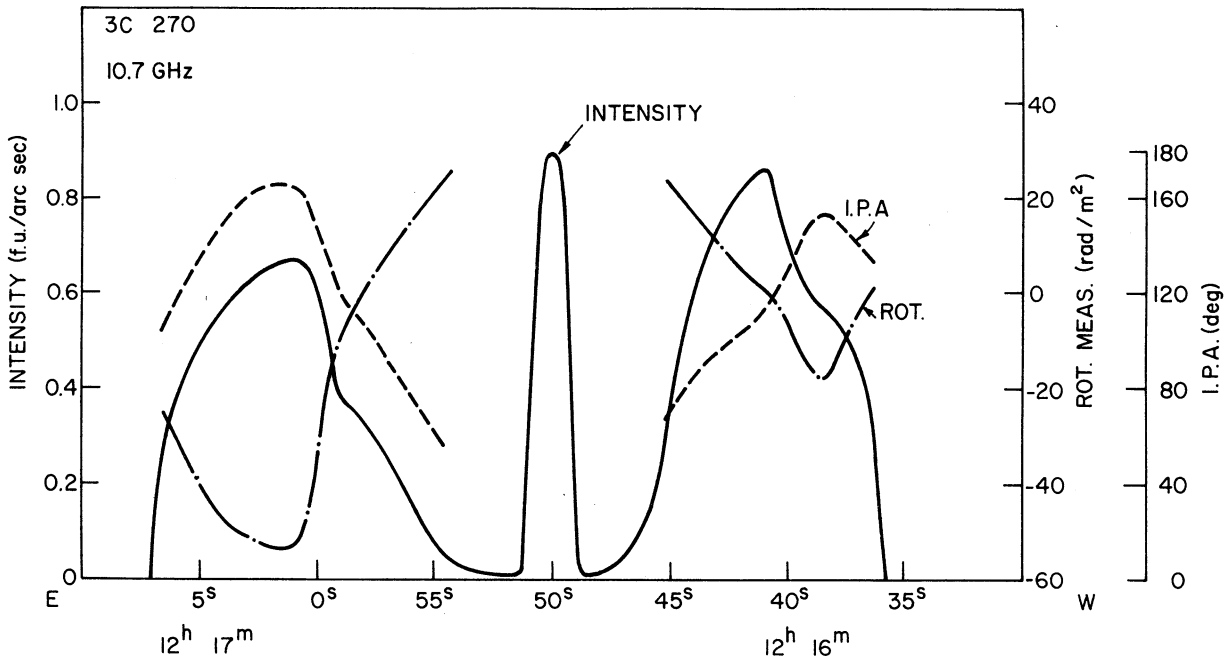

FIG. 9(c). 3C 270; Class IV-A. Intensity, rotation measure, and intrinsic position angle. Half-peak synthesized beamwidth 1.1ˢ in right ascension.

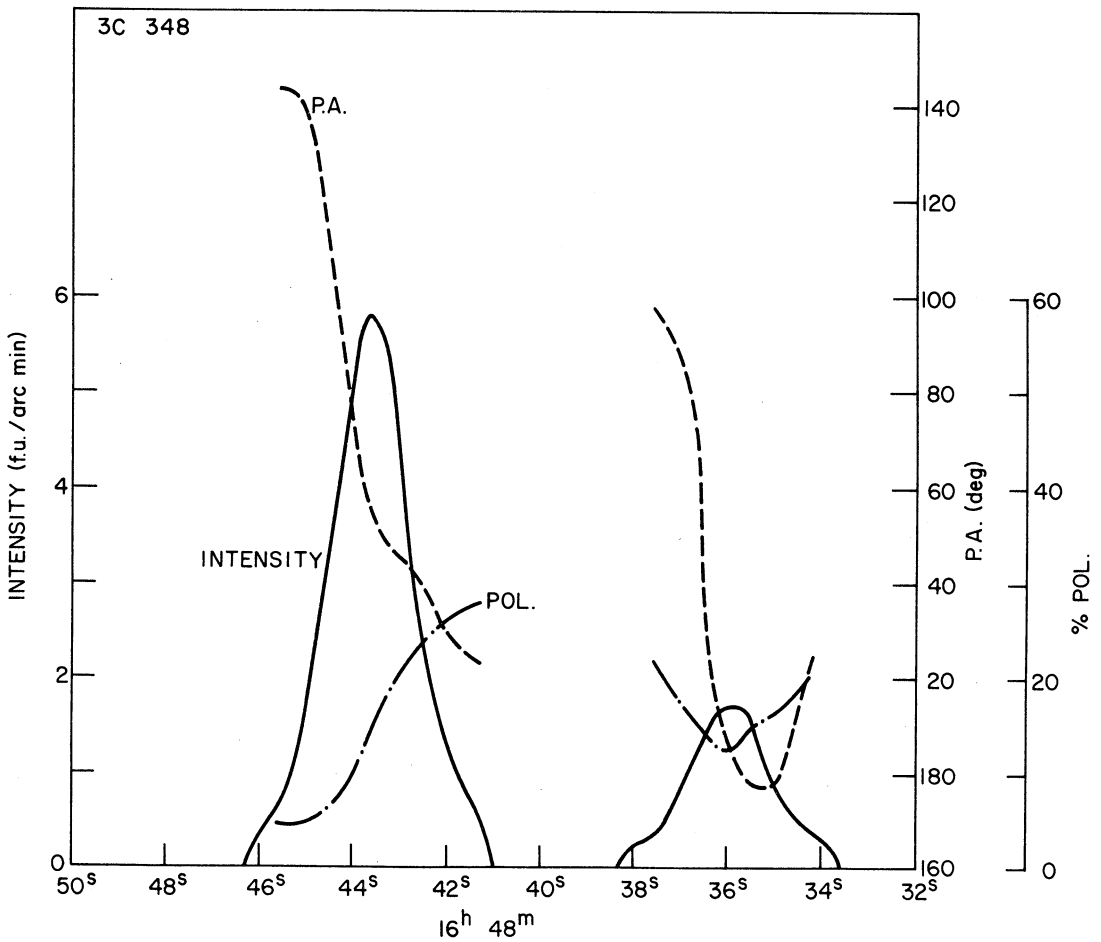

FIG. 10. 3C 348; Class IV-B. Half-peak synthesized beamwidth 1.1ˢ in right ascension.

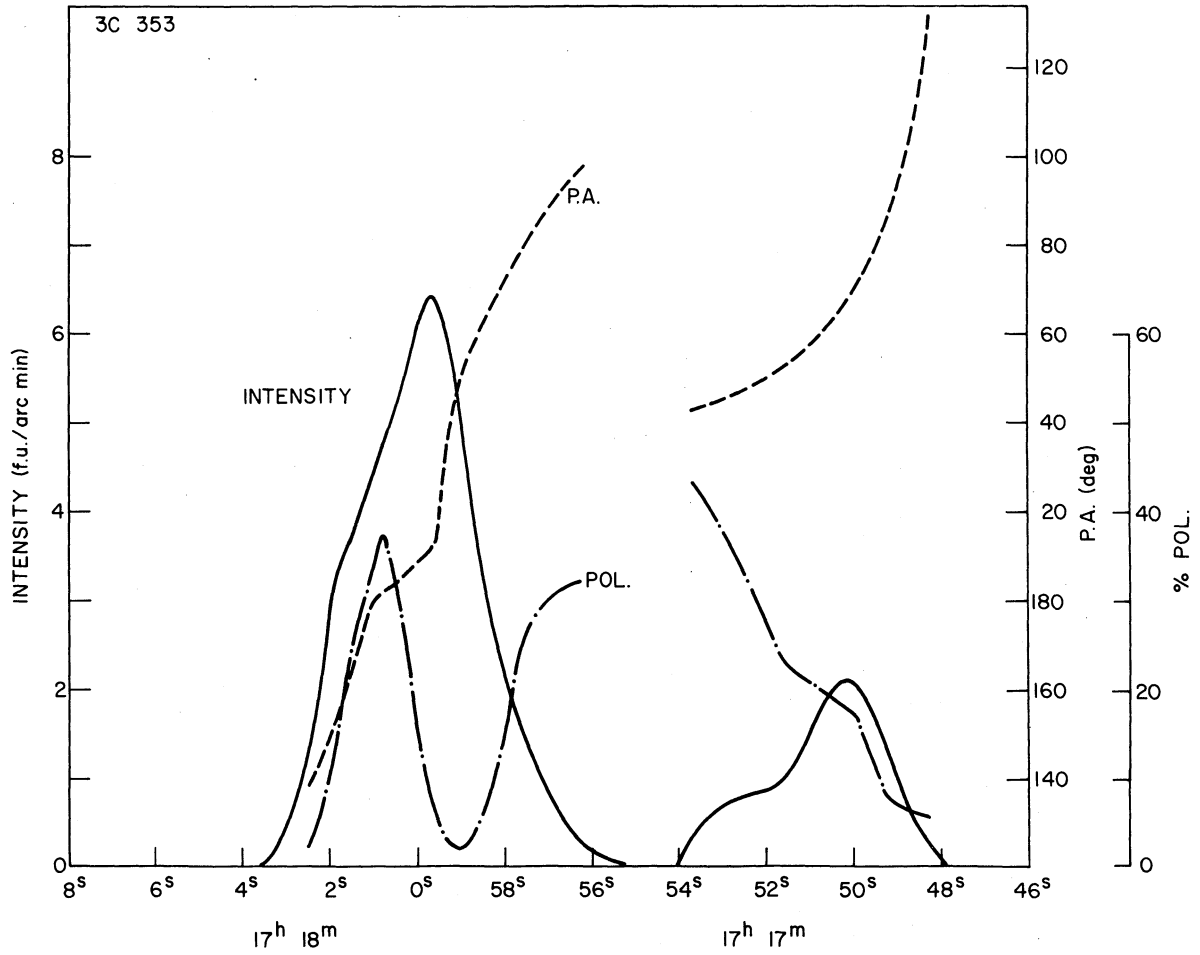

FIG. 11. 3C 353; Class IV-B. Half-peak synthesized beamwidth 1.1s in right ascension.

tion mechanism is Faraday rotation; however, at least in some sources, this cannot be the exclusive depolarization mechanism. The maximum degree of polarization that we observe for a given source is seldom greater than 40%, while in the main outer lobes of double sources maximum polarizations are generally 15%–20%. The low-frequency measurements show that in several cases, at least, depolarization takes place between 5 and 1 GHz, but that between 5 and 10 GHz there is little or no change in the degree of polarization. Yet this should be 60%–80% for an optically thin cloud of relativistic electrons with an isotropic velocity distribution and radiating by the synchrotron mechanism in a homogeneous magnetic field. If we assume that Faraday rotation is responsible for depolarization below 5 GHz, then, for those sources in which the degree of polarization fails to undergo further increase between 5 and 10 GHz, we must deduce the operation of some other mechanism to account for the discrepancy between the observed polarization values and the 60%–80% expected from theory. Probably the simplest explanation involves changes in magnetic field orientation within the source; in an optically thin emitting cloud those changes need not occur in adjacent regions of the same resolu-

TABLE VI. Data for 3C 452.

	10.7-GHz flux (f.u.)	Spectral index	Polarization 10.7 GHz (%)	Polarization 2.7 GHz (%)	Polarization 1.4 GHz (%)	Position angle 10.7 GHz (deg)	Position angle 2.7 GHz (deg)	Position angle 1.4 GHz (deg)
NE-main	0.89±0.08	−0.88	16±3	9±2	7±2	57±16	145	15
NE-tail			22±7	17±3	16±1	125±27	170	40
C	0.19±0.03	+0.23	4±3	...	...			
SW-tail	0.61±0.07	−1.12	16±8	14±3	3±2	75±40	140	135
SW-main			5±4	5±2	3±1	14±70	145	135

tion element but might take place between the front of the source, as we see it, and its rear. In the latter case improved resolving power will not result in an increase in the degree of polarization observed.

A second characteristic of the high-frequency maps is the frequent presence of a centrally located compact source in what were thought to be radio doubles. These compact sources have self-absorption spectra (flux increasing at higher frequencies), low polarization (~a few percent), and coincide with the nucleus of an optical galaxy when one can be identified. At least one (3C 111) is probably variable. Their prevalence implies that some, and perhaps all, nuclei of radio galaxies remain active throughout their lives.

V. SOURCE CLASSIFICATION

Our data strongly imply that there are at least four distinct classes of extragalactic radio sources, that there are several characteristics of both the brightness and polarization structure that vary in a systematic manner from one class to the next, and that the four possibly form an evolutionary sequence. We distinguish the compact sources (Class I), core–halo sources (Class II), triple sources (Class III), and double sources (Class IV). We point out that, as the number of sources in our sample is small and their selection not entirely free of bias (though nearly so), we do not consider this classification either comprehensive or exclusive. We cannot foreclose the possibilities that there are various subclasses, other classes, or even differing parallel sequences of classes. The claim we do make is that all 19 sources we have observed fall into a strictly limited number of categories, while these categories form a well-defined sequence. And that in itself we consider remarkable.

We mention the compact sources (Class I) for completeness only, as we did not study any in the present survey (save for 3C 66A). These are the classical quasars such as 3C 279, 3C 273, VRO 42.22.01 (BL Lacertae), and OJ 287, which are of small angular and linear diameter, show a self-absorption radio spectrum at centimeter wavelengths, exhibit a small degree of linear polarization ($<10\%$ and often $<5\%$), and are usually time variable. The remaining three classes, into which our 19 sources fall, are all of large linear dimension.

Class II sources in our sample are 3C 66B, 3C 264, 3C 274, 3C 218, 3C 433, and 3C 123. These are characterized by a bright central core and an extended halo. At centimeter wavelengths the integrated flux density of the halo is less than that of the core. The halo does not appear to be symmetrical, but is extended primarily in two opposite directions, and may broaden somewhat at great distances from the central core. One side of the halo is generally more prominent than the other, while both sides may show fine structure when observed with the highest available resolution. Halo radio spectra probably steepen at greater distances from the core; certainly these structures are most prominent at the low frequencies. The degree of linear polarization in the halos is generally high (20%–40%) at frequencies around 10 GHz, but in the two sources (3C 264 and 3C 274) for which there are good data, pronounced depolarization occurs as the observing frequency approaches 1 GHz.

The cores of the Class II sources appear, when observed with sufficient resolution, to consist of several compact components aligned along the axis of the halo in the form of a "jet," plus a quasar-like component with a self-absorption spectrum which is always coincident with the nucleus of an optical galaxy where one can be identified. The degree of polarization of the cores seems always to be small ($<10\%$), although the possibility that the small jet structures (which have spectra characteristic of optically thin synchrotron sources) are each highly polarized in differing position angles is raised by the optical data for 3C 274 (Hiltner 1959) and cannot be excluded.

There are only two examples of Class III in our sample, 3C 111 and 3C 390.3. These objects show two well-defined radio lobes on opposite sides of a central component of comparable flux density. In addition, in both sources, there is evidence for a diffuse halo-like component occupying the space along the source axis between the three bright sources; in 3C 390.3, at least, the spectrum of this diffuse component is steeper than those of the other source components. The outer lobes have virtually identical spectral indices (-0.85 and -0.86 for 3C 390.3; -0.75 and -0.67 for 3C 111). Furthermore, in both sources one of the outer components is highly polarized (~20%) at 10.7 GHz, but depolarizes by half or more as one goes to frequencies in the 1–3-GHz range, while the other component is more moderately polarized (10%–15%) at 10.7 GHz, but undergoes no significant depolarization at lower frequencies. At our resolution there does not appear to be any significant change in the degree of polarization across the outer components. The central component in 3C 111 and 3C 390.3 is quasar-like, with a self-absorption spectrum and low polarization ($\lesssim 5\%$). In 3C 111, at least, this component is probably variable.

Class IV sources superficially resemble those of Class III, but are differentiated from them by the relative flux density of the quasar-like central component at centimeter wavelengths and by the presence of highly polarized tails extending inward along the source axis from the outer components. Indeed, one can distinguish two subclasses here, Class IV-A in which the central component is merely weak compared to the two outer lobes (3C 33, 3C 270, 3C 405, 3C 452), and Class IV-B in which there is no central component at all detected at centimeter wavelengths (3C 20, 3C 98, 3C 227, 3C 348, 3C 353). One source, 3C 219, could belong to either subclass as it has a weak central component coincident with the associated optical galaxy; however,

it appears to be highly polarized, and may prove, when observed with higher resolution, to be two sources on opposite sides of the galaxy rather than a quasar-like component in its center.

All the sources we have placed in Class IV are observed to exhibit highly polarized inner tails at 10.7 GHz except 3C 227 and 3C 33. These are not necessarily anomalous. In 3C 227 the outer components do appear extended inwards, but these extensions are of such low brightness that we have not detected any fractional polarized flux, and could not detect even a relatively large one were it present. In 3C 33 the two outer components are notably more compact than those of other sources in its class and resemble those of Class III, but higher resolution than ours could show an increase in polarization toward their inner edges.

The degree of polarization in Class IV source tails ranges from about 15% to over 40%. Appreciable depolarization typically occurs at frequencies below 10 GHz but above 1 GHz, while the precise frequency varies from one source to another and even from one component of the same source to the other. In the main portions of the outer radio lobes the degree of polarization is substantially less than in the adjacent tails and typically ranges from less than 5% to nearly 20%. Unlike in the tails (and probably the halos of Class II sources), depolarization need not occur at frequencies between 10 and 1 GHz, and whether or not depolarization does take place does not seem to depend on how highly polarized the main component is.

We wish to comment on the optical identification of 3C 123. Although we barely resolve this source, we have placed it in Class II because of its highly polarized halo; however, it has been identified with an optical galaxy which, according to the high-resolution map of Mitton (1970c) and Branson *et al.* (1972), lies between the bright main component and the brightest regions of the halo to the northwest. If 3C 123 is truly the same kind of source as 3C 66B and 3C 274, then the main component should contain an opaque compact source at its core and this should be coincident with any associated optical object. Thus we speculate that the galaxy with which it is presently identified may be a foreground object proximate to the radio source by chance.

We wish finally to refer to the observations of Centaurus A (NGC 5128) previously reported by two of us (Price and Stull 1973). There we investigated the inner radio lobes and found that they contained regions where the degree of linear polarization reached 70% and other regions where it was quite low. On the basis of changes in the position angle of the plane of polarization across these regions we proposed a model for the components in which a magnetic field was everywhere parallel to the source major axis and they contained regions where the optical depth was greater than unity. None of the sources in the present sample possesses polarization structure which can be compared to that observed in the inner components of Centaurus A. We wish to point out, however, that NGC 5128 is by far the closest radio galaxy, and that were it at a distance comparable to that of the sources we have been discussing here, we would not resolve the inner components, but would see them as structure-free, highly polarized tails extending inward from the outer components. And indeed, the integrated degree of polarization of the inner lobes of Centaurus A at 10.7 GHz is comparable to that reported here for the tails of Class IV sources. We conclude that Centaurus A is a typical Class IV-A source, extremely similar in fact to 3C 270, and we speculate that the highly polarized tails of the Class IV sources are all structures in which the magnetic field is highly uniform, but where, nevertheless, the integrated degree of high-frequency polarization is reduced by the presence of optically thick condensations.

An attempt to explain the observed depolarization of the main components of Class IV sources by invoking the presence of opaque condensations fails. This is because the fact that the integrated degree of polarization in the main lobes is appreciably smaller than in the tails would require a greater proportion of the main-lobe flux to originate in the optically thick regions. However, the main lobes would then be expected to exhibit flatter spectra than the tails, but the most comprehensive data presently available (Mackay 1971) show that the opposite is true. (This is consistent with the presence of optically thick condensations in the tails, however.) Thus, if our model for the tails is correct, the magnetic field very likely becomes twisted in the main lobes, perhaps by the rotation of the central galaxy.

The four classes of radio source described here could form an evolutionary sequence, with the evolution running in either direction. We would like to propose for further consideration the possibility that progress is from Class I to Class IV as a result of the existence of a continuous or nearly continuous stream of relativistic particles flowing out in two opposite directions from a source of energy in the galactic nucleus for the entire lifetime of the radio source. We would produce the observed sequence of source classes by postulating that in the initial stages of particle ejection the density of the intergalactic medium surrounding the active object is zero or very small and that it builds up gradually as a result of the ejection. When the density is near zero, no confinement of the relativistic particles can occur, and no radio-emitting clouds will be observed at appreciable distances from the active nucleus (Class I sources). As the density increases, it is possible that a radio-emitting halo extended in the direction of the ejection will be built up (Class II sources), and finally an increasing number of thermalized particles in the vicinity of the source will begin to interact with the relativistic flow to produce well-defined radio structures (Class III sources). As the number of relativistic particles in the outer components becomes larger, they become highly luminous with respect to the nuclear source (Class IV sources). For this scheme to work, it is required that

there exist some mechanism (magnetic fields?) for decelerating at least some of the relativistic particles during the initial evolution. We do not know if detailed computations based on our proposal can give the required radio structures with the observed polarization characteristics; however, we do note the presence of double-source structure near the nucleus of at least one Class II object, 3C 274, as well as well-defined components near that of another, 3C 66B (Northover 1973). Presumably the particle density is high in these regions and accounts for the formation of such structures. Since, under our hypothesis, the observed radio-source boundaries need not correspond to boundaries of particle clouds, but might represent shocks or standing-wave patterns, our classification scheme may reflect a tendency of such shocks or wave patterns to occur at increasingly great distances from the optical object with advancing age.

VI. CONCLUSIONS

From observations of the brightnesss and polarization structure in 19 extragalactic radio sources at 10.7 GHz and comparison of our data with that available at lower frequencies, we can make the following generalizations:

(1) Many extended extragalactic radio sources possess quasar-like compact central components whose spectra indicate self-absorption at centimeter wavelengths. These components always show a low degree of polarization ($\lesssim 5\%$) and may vary in intensity.

(2) There exist at least four distinct classes of extragalactic radio sources. These classes can be arranged in a sequence in which the centimeter-wavelength flux density of the central component diminishes relative to that of the outer regions, while the structure of these outer regions becomes better organized. Each class has distinctive polarization characteristics, and the degree of polarization of the outermost source regions tends to decline along the sequence together with the relative flux density of the central source. Due to the small size of our sample, it is difficult to define subclasses, and we cannot exclude the existence of other classes or even of parallel sequences of classes.

Our four source categories are

(a) Compact sources (Class I): single, quasar-like compact source with self-absorption spectrum, low and often variable degree of polarization, and generally variable intensity.

(b) Core–halo sources (Class II): dominated by a quasar-like central source, but with an outer radio-emitting halo extending primarily in two opposite directions. The halo spectrum probably steepens at increasing distances from the core, while the polarization is high (20%–40%). Considerable depolarization usually takes place at frequencies below 10 GHz.

(c) Triple sources (Class III): the outer regions are organized into two relatively small main components whose flux density at short centimeter wavelengths is comparable to that of the compact central source. There appears to be a diffuse emission field between the core source and the outer components. The latter are moderately polarized (10%–20%) at frequencies around 10 GHz and sometimes undergo significant depolarization at lower frequencies.

(d) Double sources (Class IV): dominated by two large outer components with notable tails extended inward toward the center, but with outer edges usually sharp and well defined. The tails are highly polarized (20% to over 40%), while the main lobes are always less so (5%–20%). Both sometimes depolarize at frequencies below 10 GHz. Faraday depolarization cannot by itself account for the observed small degree of polarization in the main components, and there is likely to be considerable twisting of the magnetic field therein; however, the tails may contain a highly ordered magnetic field and optically thick condensations. Class IV may be divided into two subclasses:

(i) IV-A: the quasar-like central component is merely faint relative to the outer lobes;
(ii) IV-B: no quasar-like central component has been detected at centimeter wavelengths.

This distinction could be artificial and may not persist when observations are made at higher frequencies and to very low flux densities (i.e., 10^{-3} f.u.).

(3) These classes could form an evolutionary sequence wherein an active nucleus continuously ejects relativistic particles into an intergalactic medium of initially zero or very low density, and the radio structures in the latter classes (III and IV) arise only after the continuing ejection has built the particle density in the source vicinity to a sufficiently high level.

ACKNOWLEDGMENTS

The Stanford five-element interferometer was built with support of the Air Force Office of Scientific Research supplemented by National Science Foundation grants for equipment and design. The observations and analysis were funded by the Electrical Engineering Department of Stanford University. We thank Dr. W. Medd and Dr. G. Harvey of the National Research Council, Canada for supplying monthly 10.7-GHz flux densities of time-variable calibrator sources, and Prof. R. N. Bracewell for helpful discussions and advice.

REFERENCES

Arp, H. C. (1967). Astrophys. Lett. **1**, 1.
Baldwin, J. E., Jennings, J. E., Shakeshaft, J. R., Warner, P. J., Wilson, D. M. A., and Wright, M. C. H. (1970). Mon. Not. R. Astron. Soc. **150**, 253.
Bignell, R. C., and Seaquist, E. R. (1973). Astron. J. **78**, 536.
Bing, K. B. W., and Seielstad, G. A. (1972). Astrophys. J. **177**, 291.
Bracewell, R. N., Colvin, R. S., D'Addario, L. R., Grebenkemper, C. J., Price, K. M., and Thompson, A. R. (1973). Proc. IEEE **61**, 1249.

Bracewell, R. N., and Thompson, A. R. (1973). Astrophys. J. **182**, 77.
Branson, N. J. B. A., Elsmore, B., Pooley, G. G., and Ryle, M. (1972). Mon. Not. R. Astron. Soc. **156**, 377.
Fanaroff, B. L. (1974). Mon. Not. R. Astron. Soc. **166**, 1P.
Fomalont, E. B. (1968). Astrophys. J. Suppl. **15**, 203.
Graham, I. (1970). Mon. Not. R. Astron. Soc. **149**, 319.
Griffin, R. F. (1963). Astron. J. **68**, 421.
Grindlay, J. E., Helmken, H. F., Hanbury Brown, R., Davis, J., and Allen, L. R. (1975). Astrophys. J. To be published.
Hargrave, P. J., and Ryle, M. (1974). Mon. Not. R. Astron. Soc. **166**, 305.
Harris, A. (1972). Mon. Not. R. Astron. Soc. **158**, 1.
Hiltner, W. A. (1959). Astrophys. J. **130**, 340.
Kellermann, K. I. (1974). Astrophys. J. **194**, L135.
Kellermann, K. I., and Pauliny-Toth, I. I. K. (1973). Astron. J. **78**, 828.
MacDonald, G. H., Kenderdine, S., and Neville, A. C. (1968). Mon. Not. R. Astron. Soc. **138**, 259.
Mackay, C. D. (1969). Mon. Not. R. Astron. Soc. **145**, 31.
Mackay, C. D. (1971). Mon. Not. R. Astron. Soc. **154**, 209.
Maltby, P., and Moffet, A. T. (1962). Astrophys. J. Suppl. **7**, 141.
Mitton, S. (1970a). Astrophys. Lett. **5**, 207.
Mitton, S. (1970b). Astrophys. Lett. **6**, 161.
Mitton, S. (1970c). Mon. Not. R. Astron. Soc. **149**, 101.
Mitton, S. (1971). Mon. Not. R. Astron. Soc. **153**, 133.
Northover, K. J. E. (1973). Mon. Not. R. Astron. Soc. **165**, 369.
Price, K. M., and Stull, M. A. (1973). Nat. Phys. Sci. **245**, 83.
Riley, J. M., and Branson, N. J. B. A. (1973). Mon. Not. R. Astron. Soc. **164**, 271.
Seielstad, G. A. (1967). Astrophys. J. **147**, 24.
Seielstad, G. A., and Weiler, K. W. (1969). Astrophys. J. Suppl. **18**, 85.
Seielstad, G. A., and Weiler, K. W. (1971). Astron. J. **76**, 211.